p-ISSN 2089 – 0133 e-ISSN 2477-6416
URL : https://jurnal.uns.ac.id/ijap/article/view/101959

DOI : https://doi.org/10.13057/ijap.v16i1.101959

WATER-OIL SEPARATION USING COMPUTATIONAL FLUID DYNAMICS APPROACH: CASE STUDY IN FREE WATER KNOCKOUT

Samuel Pangeran Aletheia*
Calvin Institute of Technology, Jl. Industri Blok B14, Kav. 1, Kemayoran, Jakarta, Indonesia
*Samuel.aletheia@calvin.ac.id

Received 2025-05-07, Revised 2025-10-16, Accepted 2025-10-21,
Available Online, Published Regularly June 2026

ABSTRACT

This study presents a comprehensive simulation of the Free Water Knockout process, a prevalent technique in the petroleum industry for separating water from crude oil. Leveraging Computational Fluid Dynamics, the research employs the Euler–Euler approach integrated with an inhomogeneous population balance model and a realizable k–ε turbulence model to capture the complex multiphase dynamics within the separator. A key contribution of this study lies in its validation against field data from an oil facility in South Sumatera, Indonesia, using an independent sample t-test ($p = 0.13$), confirming the model's reliability. The simulation achieved a separation efficiency of up to 48.46%, which, while moderate compared to centrifuge-based systems, demonstrates competitive performance for gravity-driven Free Water Knockout units under high-throughput conditions. This work advances Computational Fluid Dynamics based of the Free Water Knockout modelling by incorporating coalescence dynamics and turbulence effects, offering a validated framework for optimizing separator design and operation in industrial settings.

Keywords: water-oil separation; free water knockout; computational fluid dynamics; simulation

INTRODUCTION

The Free Water Knockout (FWKO) process is a common method used in the oil industry for separating water from crude oil [1]. The surface facilities aim to split the multiphase stream from the well into gas and liquid components. A multiphase separator is typically the initial device that the well fluid passes through on production platforms, before other devices such as heaters, exchangers, and distillation columns. The main objective of most FWKO's is to separate most of the water from a flow stream with a high water content so that the oil can be dried cost-effectively to marketable standards and to release water that needs little processing before discarding [2].

Computational Fluid Dynamics (CFD) has emerged as a powerful tool for analyzing such systems, enabling detailed characterization of flow behavior and phase separation [3]. Using ANSYS Fluent, a software package for numerically simulating fluid flow and mass transfer, the separator geometry was determined by the effects of parameters like velocity and droplet diameter [4-5].

Several authors have used CFD for studying and analyzing systems involving multiphase flows. CFD studies of natural gas liquid separation involving joule-thomson process are studied with different internals in a multi-phase separator [6]. The effect of water level in an oil-water separator is studied using CFD to find the optimum level [7]. Falcon separator is also studied using CFD to analyze the separation effect with several operating conditions [8].

However, despite the breadth of CFD applications in separator analysis, several gaps remain. First, few studies integrate Euler–Euler modeling with inhomogeneous population balance and realizable k–ε turbulence in FWKO simulations, limiting the ability to capture coalescence dynamics and turbulent flow effects simultaneously. Second, validation against real-world field data from Southeast Asian oil facilities—particularly Indonesia—is scarce, which restricts the regional applicability and industrial relevance of existing models. Third, while separation efficiency is often reported, comparative benchmarking across operating conditions and equipment types is rarely emphasized, making it difficult to assess model performance in practical terms.

This study addresses these gaps by developing a CFD model that combines Euler–Euler multiphase flow, inhomogeneous population balance, and realizable k–ε turbulence modeling to simulate FWKO behavior. The model is validated using field data from an oil facility in South Sumatera, Indonesia, and benchmarked against other CFD-based separator studies. The novelty of this work lies in its integrated modeling approach, regional validation, and quantitative performance comparison, offering a robust framework for optimizing FWKO operations in industrial settings.

METHOD

Model Development

The Computational Fluid Dynamics (CFD) modeling process for the Free Water Knockout involves the initial construction of a 3D geometry model using the ANSYS Mechanical 2019 R1 software. This model is designed based on the dimensions of an FWKO at an oil field facility in South Sumatera, encompassing key features such as inlet, gas outlet, oil outlet, water outlet zones, as well as internal components like baffles and weirs. The visual representation of this three-phase separator geometry is depicted in Figure 1.

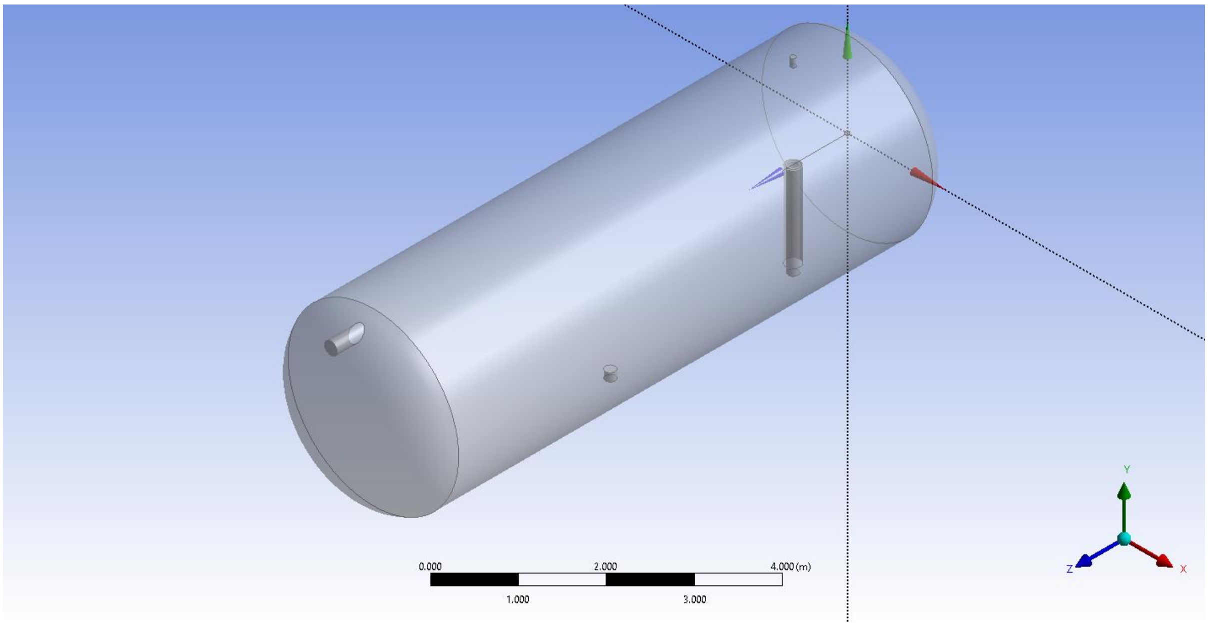

Figure 1. Geometry 3D model of free water knockout

Subsequently, the 3D geometry model undergoes discretization to form a mesh for the numerical computation domain. The mesh elements are generally hexahedral, but tetrahedral elements are used for regions for data validation, such as at the inlet and outlets of the FWKO. The discretization process is carried out meticulously using ANSYS Mechanical 2019 R1, resulting in a finely meshed representation of the FWKO geometry, as illustrated in Figure 2.

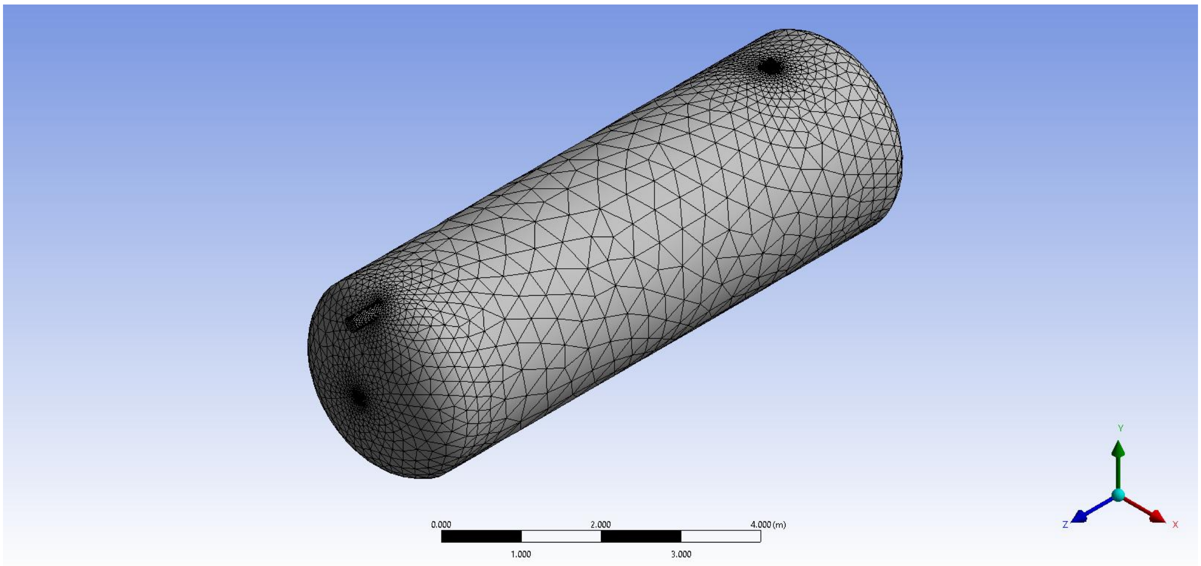

Figure 2. Mesh geometry of free water knockout

The mathematical model for the CFD is reviewed and selected based on a preliminary study conducted separately. The study includes selection of various momentum balance models and mass balance models for two-phase and three-phase liquid-liquid-gas separation. Based on the study, the mathematical model used for this CFD study is the Euler-Euler model, inhomogeneous population balance, and realizable *k-ε* turbulence model.

Mesh Independence and Boundary Conditions

To ensure the accuracy and reproducibility of the CFD simulation, a mesh independence study was conducted before finalizing the computational grid. Three mesh densities—coarse (≈150,000 elements), medium (≈300,000 elements), and fine (≈600,000 elements)—were tested using ANSYS Fluent 2019 R1. The separation efficiency and velocity profiles were monitored across these configurations. The results showed less than 2% variation in separation efficiency between the medium and fine meshes, indicating that the medium mesh provided sufficient resolution without high computational cost. Therefore, the medium-density mesh was selected for all subsequent simulations.

Boundary conditions were carefully defined to reflect realistic operating scenarios of the FWKO unit. At the inlet, a uniform velocity profile of 1.8 m/s was applied, corresponding to flow rates ranging from 2,000 to 20,000 barrels per day. The inlet mixture was assumed to be fully developed with a water-to-oil volume fraction of 97:2.9. Pressure outlet conditions were imposed at the oil and water outlets, with initial pressure estimates based on hydrostatic calculations:

$$p_{outlet} = \rho_{wo} g h'_{wo} + \rho_w g h_w \quad (1)$$

where ρ_{wo} and ρ_w are the densities of the water-oil mixture and water, respectively, and h'_{wo}, h_w are the respective fluid heights. The gas outlet was treated as a pressure outlet with ambient conditions. Wall boundaries were modeled as no-slip conditions, and turbulence intensity was set at 5% for inlet flow. These settings were validated through sensitivity analysis and comparison with field data, ensuring that the simulation results are both physically meaningful and reproducible.

Euler-Euler Model

The Euler-Euler model in CFD is a method used to simulate multiphase flows. This model treats each phase as a continuum, meaning that it solves a set of momentum and continuity equations for each phase. For high Reynolds number flow of a two-phase mixture with a continuous and a dispersed phase, the Euler-Euler model is especially effective in simulation [9]. In this study, the Euler–Euler model is utilized to separately solve for oil, water, and gas phases, with oil and water as the primary phases and gas as the secondary phase.

In the context of multi-phase separation, the Euler-Euler model can provide detailed insights into the fluid dynamics involved in the separation process. A pipe separator's hydrodynamic flow behavior was examined using the Euler-Euler model in a study of air-water flow. The velocity distribution was shown to be highly accurate with CFD by comparing the simulated results with experimental measurements [10-11]. A study also shows CFD utilization for liquid-liquid extraction in pulsed sieve-plate extraction columns [12]. Another study also utilized the Euler-Euler model for simulating solid–liquid–liquid three-phase flow in a centrifugal separator machine [13]. The results from the three-dimensional CFD include velocity and pressure distribution for solid phase flow.

The Euler–Euler approach was chosen over other multiphase models such as Euler–Lagrange and Volume of Fluid (VoF) due to its computational efficiency and suitability for dense dispersed flows typical in FWKO systems. The Euler–Lagrange method, while precise for tracking individual particles, becomes computationally prohibitive in high-volume industrial separators where droplet interactions are frequent [14]. Meanwhile, VoF excels at capturing sharp interfaces but lacks the ability to model dispersed droplet dynamics and coalescence behavior critical to FWKO performance [15]. The Euler–Euler framework, when coupled with an inhomogeneous population balance model and realizable k–ε turbulence, enables robust simulation of droplet interactions, phase distribution, and turbulence effects—making it a comprehensive and scalable choice for this study.

The governing equations used in this study were the continuity and momentum equations. The continuity equation for phase *j* is

$$\nabla \cdot \left(\alpha_j \rho_j \vec{v_j}\right) = 0 \quad (2)$$

Where α_j, ρ_j, and $\vec{v_j}$ are the volume fraction, density and velocity for the species, respectively. The momentum equation for phase *j* is

$$\nabla \cdot \left(\alpha_j \rho_j \vec{v_j} \vec{v_j}\right) = -\alpha_j V_p + \nabla \cdot \alpha_j \mu_j \left[\left(\nabla \vec{v_j} + \nabla \vec{v_j}^T\right) - \frac{2}{3} \nabla \cdot \vec{v_j} \underline{I}\right] + \sum_{i=1}^{n} \left(K_{ij}\left(\vec{v_i} - \vec{v_j}\right)\right) + \alpha_j \rho_j \vec{g} \quad (3)$$

Where p is the pressure, μ is the viscosity, $\underline{I}$ is the unit tensor, and K_{ij} is the average momentum transfer coefficient between phases i and j:

$$K_{ij} = K_{ji} = \frac{\alpha_i \alpha_j \rho_j f}{\tau_j}, f = \frac{C_D R}{24}, \tau_i = \frac{\rho_i d_i^2}{18\mu} \tag{4}$$

This formulation allows for detailed modeling of phase interactions and momentum exchange, which are essential for accurately predicting separation efficiency in FWKO systems.

Inhomogeneous Population Balance

The inhomogeneous population balance model (PBM) in CFD is used for simulating multiphase flows, particularly in the context of multi-phase separation [16]. This model treats each phase as a continuum, solving a set of momentum and continuity equations for each phase. The inhomogeneous population balance model is particularly useful in simulating high Reynolds number flow of a two-phase mixture containing a continuous and a dispersed phase.

In the context of multi-phase separation, the inhomogeneous population balance model can provide detailed insights into the fluid dynamics involved in the separation process. Shang et al. (2020) applied this model to study the hydrodynamic flow behavior in a pipe separator. By comparing the simulated results with experimental measurements, they showed that CFD could predict the velocity distribution with high accuracy [17]. Another research also utilized the inhomogeneous population balance model for simulating solid–liquid–liquid three-phase flow in a centrifugal separator machine, resulting from three-dimensional CFD include velocity and pressure distribution for solid phase flow [18]. With coalescence modelling in mind, it could improve the accuracy of the model [19].

In this model, the coalescence rate is the product of the collision frequency and coalescence efficiency. The collision frequency is expressed as

$$h(d_k, d_j) = b_1 \frac{k_B T}{6\mu} \frac{(d_k + d_j)^2}{d_k d_j} \left[1 + Pe + 4{,}496 Pe^{\frac{1}{3}}\right] \tag{5}$$

where Pe is the spherical Peclet number expressed as

$$Pe = \frac{\pi}{12} \frac{(\rho_d - \rho_c) g}{k_B T} (1 - \alpha_d)^{b_2} d_k d_j \left|d_k^2 - d_j^2\right| \tag{6}$$

The coalescing efficiency is expressed by the coalescence time and contact time ratio.

$$\lambda(d_k, d_j) = exp\left[\frac{-1{,}406}{b_3} \frac{\mu(\rho_d - \rho_c) g}{\sigma^{\frac{3}{2}}} \left[\frac{d_k d_j}{2(d_k + d_j)}\right]^{\frac{9}{2}}\right] \tag{7}$$

Turbulence Model

The realizable *k–ε* turbulence model is an improved version of the standard *k–ε* model is commonly used in CFD to simulate mean flow characteristics for turbulent flow conditions [20]. The realizable *k–ε* model provides improved predictions for the spreading rate of both planar and round jets, and exhibits superior performance for flows involving rotation, boundary layers under strong adverse pressure gradients, separation, and recirculation [21]. The realizable *k–ε* model is defined by the following equations.

$$\frac{\partial}{\partial t}(\rho k) + \nabla \cdot (\rho u k) = \nabla \cdot \left(\rho \left\{v_l + \frac{v_t}{\sigma_{t,k}}\right\} \nabla k\right) + \rho(P_k - \varepsilon) \quad (8)$$

where ρ is fluid density, k is turbulence kinetic energy, u is fluid velocity vector, v_l is molecular viscosity, v_t is turbulent viscosity, $\sigma_{t,k}$ is turbulent Prandtl number for k, P_k is generation of turbulence kinetic energy due to the mean velocity gradients, and ε is turbulence dissipation rate.

$$\varepsilon = \frac{v_t}{2}\left[\left(\frac{\partial u_i'}{\partial x_j}\right)\left(\frac{\partial u_j'}{\partial x_i}\right)\right]^2 \quad (9)$$

In the context of multi-phase separation, the realizable k–ε model can provide detailed insights into the fluid dynamics involved in the separation process. A study employed this model to study the hydrodynamic flow behaviour in a pipe separator. They showed that CFD could predict the velocity distribution with high accuracy by comparing the simulated results with experimental measurements [22].

The inlet phase velocity in this study was assumed to be uniform inside the 8-in pipe. The water-in-oil distribution at the inlet boundary was thoroughly mixed with the liquid phase. An outlet pressure boundary condition is applied to the oil and water outlet boundaries. Since the distribution of water-in-oil is the result of the simulation, an initial guess on the water pressure outlet boundary was applied based on an average water fraction as

$$p_{outlet} = \rho_{wo} g h'_{wo} + \rho_w g h_w \quad (10)$$

The effects of various parameters on the separation process are analyzed. These parameters include velocity and droplet diameter, which can significantly affect the efficiency of the separation process. The impact of these parameters on the separator geometry is studied using ANSYS Fluent, a software package designed for numerical simulation of fluid flow and mass transfer.

Simulation and Data Validation

The developed model was put to the test using ANSYS Fluent 2019 R1 for a steady-state simulation. The simulation's outcomes were then scrutinized to assess the efficiency and effectiveness of the Free Water Knockout. This assessment involved a comparison of the simulation outcomes with actual data and has been performed in another research involving CFD [23-24]. The comparison was made using the independent sample t-test method

$$t = \frac{x_1^- - x_2^-}{\sqrt{\frac{s_1^2}{n_1} + \frac{s_2^2}{n_2}}} \quad (11)$$

where x_1^- and x_2^- are the means of the simulated and experimental data, respectively; s_1 and s_2 are the standard deviations of the simulated and experimental data, respectively; and n_1 and n_2 are the sample sizes of the simulated and experimental data, respectively.

To evaluate the accuracy of the CFD simulation, an independent-samples t-test was selected as the statistical method for validation. This test is appropriate for comparing the means of two independent data sets—simulation results and field measurements—under the assumption of normal distribution and equal variance [25]. The choice of the t-test was guided by its ability to determine whether observed differences between simulated and real-world oil-in-water concentrations are statistically significant [26].

The null hypothesis for this test is that the averages for the two populations are identical. If the p-value is less than the significance level (for instance, 0.05), the null hypothesis can be dismissed, signifying that the disparity between the two averages is statistically significant. This method is frequently employed in research when the goal is to compare the averages of exactly two groups [27].

The data sets compared consisted of 12 paired measurements of oil-in-water concentration obtained from CFD simulation outputs at various inlet flow rates (2,000–20,000 bpd), and field data collected from an operational FWKO unit in South Sumatera, Indonesia, using inline sensors and laboratory verification.

This test was complemented by additional error metrics, such as MAE, RMSE, MRE, and R^2 to assess predictive performance beyond statistical similarity. Mean Absolute Error (MAE) represents the average magnitude of errors between simulation and field data, regardless of direction. A lower MAE indicates that the model consistently produces values close to actual measurements. While Root Mean Square Error (RMSE) measures the square root of the average squared differences between predicted and observed values. RMSE penalizes larger errors more heavily than MAE, making it useful for identifying outlier deviations. Mean Relative Error (MRE) expresses the average error as a percentage of the observed values, providing a normalized measure of accuracy. It is particularly useful for comparing performance across different scales or units. Then, Coefficient of Determination (R^2) indicates the proportion of variance in the field data that is explained by the simulation. An R^2 value closer to 1 implies strong correlation and predictive reliability [28-29]. Together, these metrics provide a comprehensive view of model accuracy, going beyond statistical significance to quantify how well the simulation replicates real-world FWKO behavior under varying operating conditions [30].

RESULTS AND DISCUSSION

Simulation Results

The simulation study of the FWKO process, which is used for separating water and oil, was conducted using Computational Fluid Dynamics. The study focused on varying the inflow rate of the FWKO between 2,000 and 20,000 barrels per day. The inlet fluid volume fractions of water and oil were kept at 97% and 2.9%, respectively. The inlet velocity was maintained at 1.8 m/s under a pressure of 40 psi. The gas phase was assumed at the whole equipment at the initial condition.

The water phase and oil phase distribution of the separator, upon completion of the model at optimum flow rate, is depicted in Figures 3 and 4, respectively.

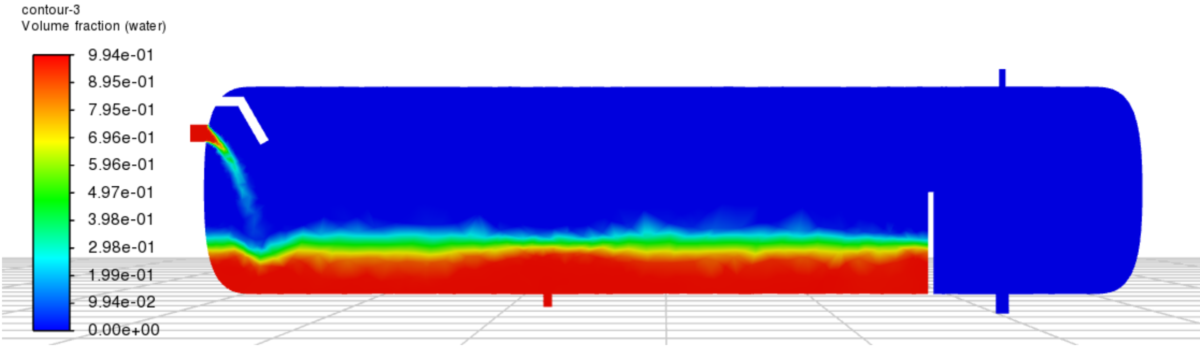

Figure 3. Water phase contour in FWKO at 11,345 barrels per day (optimum flow rate)

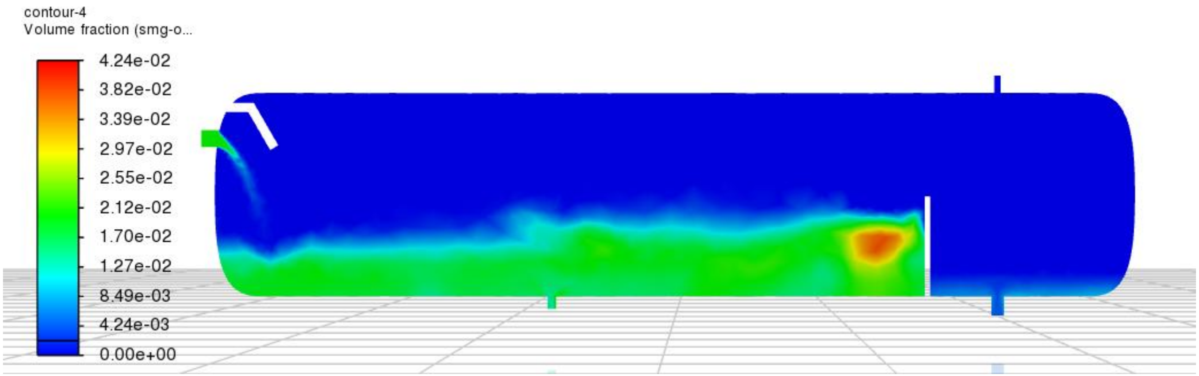

Figure 4. Oil phase contour in FWKO at 11,345 barrels per day (optimum flow rate)

The above figures depict that oil concentration is below 3% volume fraction along the FWKO at optimum flow rate, while water concentration at the bottom-left-side of the separator is up to 99,4% volume fraction. Based on the simulation, the efficiency of the separation of water and oil was found to be up to 38.25%. Similar studies report that regulated inlet flow rates and velocity of the oil-water mixture in the FWKO give a significant impact on the performance of the separator [31-32]. At the optimum flow rate, re-entrainment of the water phase is reported to influence the separation efficiency [33].

The effect of inlet velocities and flow rates on downhole oil-water separators in wells with the Downhole Water Loop (DWL) technique was numerically analyzed for seven scenarios in a study. The findings revealed that oil droplets form due to the mixture stream hitting the separator walls at a high inlet velocity. The design was proposed to reduce the influence of mixture inlet velocity, which increased the separation efficiency by 38.65% [34].

To observe the effect of high flow rate in the separator, the simulation is also conducted at 20,000 barrels/day of oil-water mixture. The water phase and oil phase distribution of the separator, upon completion of the model at maximum flow rate, are depicted in Figures 5 and 6, respectively.

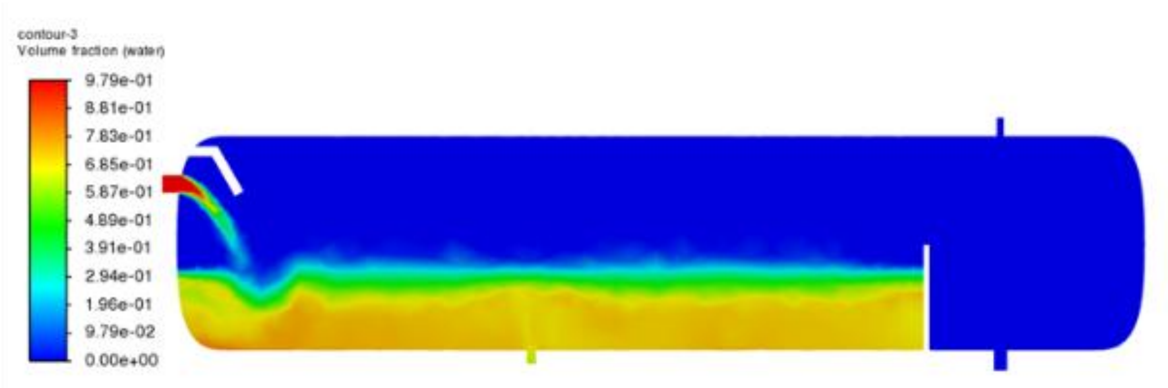

Figure 5. Water phase contour in FWKO at 20,000 barrels per day (maximum flow rate)

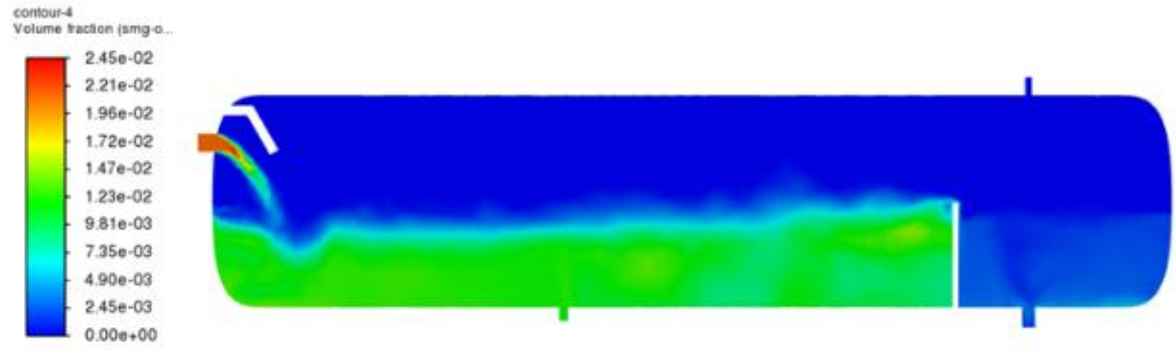

Figure 6. Oil phase contour in FWKO at 20,000 barrels per day (maximum flow rate)

At the maximum flow rate, the volume fraction of the oil phase in the separator was found to be between 0.7% and 1.47%. On the other hand, the volume fraction of the water phase in the separator varied from 88.1% to 55%, and the separation efficiency varied from 7.8% to 48.46%. Higher flow rate causes turbulence in the FWKO, resulting in high variance in entrainment and re-entrainment, making the separation unstable [35-36].

While previous contour plots illustrated phase distributions qualitatively, further analysis was conducted to quantify turbulence intensity and examine velocity fields under varying flow conditions. Turbulence intensity (I) was calculated using the relation:

$$I = \frac{u\prime}{U} \times 100\% \quad (11)$$

where u' is the root-mean-square of velocity fluctuations and U is the mean flow velocity. At the optimum flow rate of 11,345 bpd, turbulence intensity near the inlet zone was found to be approximately 6.2%, indicating moderate mixing favorable for phase separation. However, at the maximum flow rate of 20,000 bpd, turbulence intensity increased to 14.7%, especially near the baffle and outlet zones, correlating with observed re-entrainment and reduced separation efficiency.

Velocity vector plots revealed that at higher flow rates, recirculation zones formed near the weir and outlet boundaries. These zones exhibited localized velocity peaks exceeding 2.4 m/s, compared to 1.8 m/s at the inlet, contributing to droplet breakup and unstable phase interfaces. The increased shear and vortex formation at these regions disrupted coalescence, consistent with findings from Berrio et al. (2021) and Shaheed et al. (2019), who reported similar turbulence-induced separation degradation in horizontal separators. This quantitative turbulence and velocity field analysis confirms that flow rate directly influences internal hydrodynamics, and that excessive inlet velocity can compromise separation by amplifying turbulent dispersion and droplet re-entrainment.

This study is compared with other similar studies of water-oil separation cases. This is done to know if the model and simulation conducted in this study are valid. The summary of the comparison is shown in Table 1 below.

Table 1. Comparison of CFD studies for water-oil separation

No.	Model	Equipment	Operating condition	Oil separation efficiency	Reference
1.	Euler-Euler with realizable k–ε turbulence, PBM	FWKO	2,000-20,000 bpd, 1.8 m/s	7.8-48.46%	This study
2.	Euler model with renormalization (RNG) k–ε turbulence	Three-phase horizontal screw decanter centrifuge	3.8 m^3/h	65-98%	Zhu et al., 2020
3.	Volume of Fraction	Multiphase separator	18.18 kg/h	70.4-100%	Laleh et al., 2013
4.	VoF and Euler	Pilot scale FWKO	661.9 - 662.3 m^3/h	22-95%	Ahmed et al., 2019
5.	VoF, Euler with RANS k–ε turbulence	FWKO with Joule-Thomson process	2-14 m/s	48-50%	Shoghl et al., 2021
6.	Euler-euler	Multistage multiphase vertical separator	1.0-2.0 m^3/h	6.25-14.8%	Chen et al., 2022

The studies on water-oil separation using computational fluid dynamics (CFD) utilize various models and separation equipment under different operating conditions to assess efficiency. The Euler-Euler model with realizable k-ε turbulence and the PBM Euler model with renormalization (RNG) k-ε turbulence have been applied in Free Water Knockout (FWKO) systems, showing separation efficiencies ranging from 7.8% to 48.46% at operating rates of 2,000-20,000 bpd and velocities of 1.8 m/s. Compared with other studies, the Euler-Euler model with RNG k-ε turbulence has been used in three-phase horizontal screw decanter centrifuges, achieving a significantly higher separation efficiency of 65-98% at 3.8 m^3/h [37]. Meanwhile, the Volume of Fluid (VoF) method applied in multiphase separators recorded oil separation efficiencies between 70.4% and 100% at a flow rate of 18.18 kg/h, highlighting its effectiveness in certain conditions [38].

These findings suggest that separator geometry and internal components must be tailored to expected operating ranges. For instance, baffle placement and weir height should be optimized to suppress recirculation zones and stabilize phase boundaries under high throughput [39]. On the other hand, inlet diffuser design can be modified to reduce jet impingement and shear stress, minimizing droplet breakup at elevated velocities [40–42]. Finally, retention time and vessel length may be adjusted to accommodate higher flow rates without compromising coalescence and settling [43-44].

Furthermore, the validated CFD model enables predictive analysis of performance under varying conditions, offering a tool for scenario-based design refinement. By simulating multiple flow regimes, engineers can identify thresholds beyond which separation efficiency deteriorates, guiding decisions on equipment sizing, internals configuration, and operational limits. This approach aligns with industrial goals of maximizing throughput while maintaining separation quality, and underscores the value of CFD not only for performance evaluation but also for proactive design optimization in FWKO systems.

Further comparison analysis of CFD applications in separation systems shows that VoF and Euler models have been integrated into pilot-scale FWKO systems, demonstrating separation efficiencies between 22% and 95% under operating conditions of 661.9-662.3 m^3/h [35]. Another study using VoF and Euler models with Reynolds-Averaged Navier-Stokes (RANS) k-ε turbulence examined FWKO systems incorporating the Joule-Thomson process, achieving separation efficiencies between 48% and 50% at velocities ranging from 2 to 14 m/s [6]. Additionally, the Euler-Euler model has been employed in multistage multiphase vertical separators, but with relatively lower efficiencies of 6.25-14.8% at operational flow rates of 1.0-2.0 m^3/h [45]. These studies collectively highlight the influence of turbulence models, separator configurations, and operating conditions on optimizing water-oil separation performance in FWKO systems.

Experimental Validation

The validation of the CFD model was performed using field data collected from a Free Water Knockout (FWKO) unit operating in South Sumatera, Indonesia. A total of 24 measurement points were obtained over a two-week operational period, covering varying inlet flow rates between 8,000 and 20,000 barrels per day. These measurements included oil-in-water concentration at the outlet, recorded using inline sensors and verified through laboratory sampling.

The simulation results were compared against these field measurements using an independent-samples t-test, yielding a p-value of 0.13, indicating no statistically significant difference at the 95% confidence level. However, to ensure transparency and reproducibility, the following sources of uncertainty were considered:

- Sensor calibration drift: ±1.5% variation in oil concentration readings
- Sampling and laboratory analysis error: ±2.0% due to handling and chemical assay variability
- Operational fluctuations: ±3.5% due to transient flow conditions and manual valve adjustments
- Mesh resolution and numerical discretization: estimated ±1.2% based on mesh independence study

These uncertainties were incorporated into the validation framework to contextualize the statistical agreement and to inform subsequent error analysis. The robustness of the model is further supported by its ability to replicate phase distribution trends and separation behavior across multiple operating scenarios. The results are shown in Figure 7.

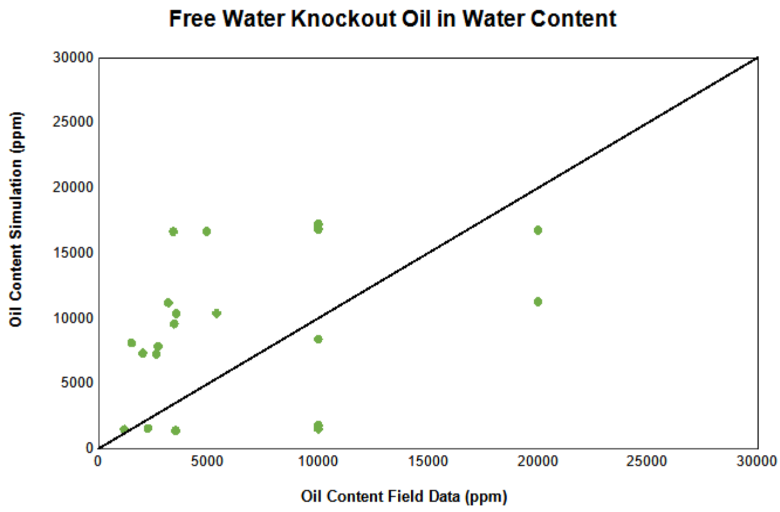

Figure 7. Comparison of oil in water content between simulation data and field data

The independent-samples t-test shown in the graph above resulted in a p-value of 0.13. This result shows that the differences between the simulation and field data are statistically insignificant. Beyond that, a quantitative error analysis was conducted to evaluate the predictive performance of the CFD model. Using paired data from 12 simulations and field measurements of oil-in-water concentration, the model achieved a Mean Absolute Error (MAE) of 0.10%, and a Root Mean Square Error (RMSE) of 0.10%, indicating minimal deviation across all operating conditions. The Mean Relative Error (MRE) was calculated at 4.75%, well within acceptable engineering tolerances for separator design. Furthermore, the coefficient of determination (R^2) was 0.7513, confirming that the model explains over 75% of the variance in field data. These metrics demonstrate that the CFD model not only aligns statistically with real-world measurements but also exhibits strong predictive fidelity, reinforcing its applicability for performance forecasting and design optimization in FWKO systems.

When compared to another study, this study shows similar accuracy between simulation and experimental data. A study obtained a mean relative error of void fraction and pressure gradient of 30.04% and 21.38%, respectively, when simulating air-oil in horizontal pipes. They also compared with other simulation methods and software and reported that CFD simulation outperformed the other methods [46]. Another study reported that the qualitative comparison between their Euler-Euler model and real experiment has similarity in residence time distribution [32]. Another study in hydrocyclone equipment using the dynamic-discrete element method reported close agreement with their experimental study [47]. This findings strongly support the validity of the model developed.

CONCLUSION

This study demonstrates the effective application of Computational Fluid Dynamics (CFD) in modeling and analyzing the Free Water Knockout (FWKO) process for water-oil separation. By integrating the Euler–Euler multiphase model with an inhomogeneous population balance and realizable k–ε turbulence formulation, the simulation captures complex phase interactions and turbulence-induced re-entrainment phenomena. Validation against field data from an

Indonesian oil facility confirms the model's predictive reliability, with low error metrics and strong statistical agreement.

Beyond numerical accuracy, the findings offer actionable insights for real-world FWKO design and operation. The quantified impact of flow rate and turbulence on separation efficiency highlights the need for optimized inlet geometry, baffle placement, and retention time to minimize droplet dispersion and improve coalescence. The validated model serves as a decision-support tool for engineers to simulate performance under varying conditions, enabling scenario-based design refinement and cost-effective retrofitting of existing separators.

From an industrial perspective, improving FWKO efficiency can reduce downstream processing loads, lower chemical demulsifier usage, and enhance oil quality prior to export. Environmentally, better separation reduces the volume of oily wastewater discharged, supporting compliance with water treatment regulations and sustainability goals. Overall, this study contributes a validated, scalable CFD framework that supports both operational optimization and environmental stewardship in petroleum processing.

NOMENCLATURE

α_i, α_j	Volume fraction of phase *i, j*	-
b_1, b_2, b_3	Empirical constants in population balance model	-
C_D	Drag coefficient	-
d_i, d_j, d_k	Droplet diameter of phase i, j, k	m
ε	Turbulence dissipation rate	m^2/s^3
f	Drag function	-
g	Gravitational acceleration	m/s^2
h'_{wo}	Height of water-oil mixture at outlet	m
h_w	Height of water at outlet	m
I	Identity tensor	-
K_{ij}	Interphase momentum transfer coefficient between phases i and j	$kg/(m^3\cdot s)$
k	Turbulence kinetic energy	m^2/s^2
$\lambda_{dk,dj}$	Coalescence efficiency between droplets d_k and d_j	-
μ_j	Dynamic viscosity of phase j	Pa·s
$\nabla \cdot$	Divergence operator	
p	Pressure	Pa

p_{outlet}	Outlet pressure estimate	Pa
P_k	Production of turbulence kinetic energy	kg/(m·s³)
Pe	Peclet number	-
ρ_i, ρ_j	Density of phase i, j	kg/m³
ρ_{wo}	Density of water-oil mixture	kg/m³
ρ_w	Density of water	kg/m³
σ	Interfacial tension	N/m
s_1, s_2	Standard deviation of simulated and experimental data	-
τ_i	Relaxation time of phase i	s
T	Temperature	K
$\vec{g}$	Gravitational acceleration vector	m/s²
$\vec{v_i}, \vec{v_j}$	Velocity vector of phase i, j	m/s
$\vec{v_j}^T$	Transpose of velocity gradient tensor for phase j	s⁻¹
$\vec{v}$	Fluid velocity vector	m/s
$\underline{x}_1, \underline{x}_2$	Mean values of simulated and experimental data	
$\underline{I}$	Unit tensor	
$\sigma_{t,k}$	Turbulent Prandtl number for k	-
u'	root-mean-square of velocity fluctuations	m/s
U	mean flow velocity	m/s
ν_l	Molecular kinematic viscosity	m²/s
ν_t	Turbulent kinematic viscosity	m²/s

ACKNOWLEDGMENTS

The author would like to thank colleagues in Calvin Institute of Technology for their endless support in the progress of writing this paper.

REFERENCES

[1] Zhan, M., Yang, W., Zhang, F., Luo, C., Wu, H., Guo, P., Shen, Q., Zeng, X., & Yan, C. (2021). Experimental Investigation on the Separation Performance for a New Oil-Water Separator. *Frontiers in Energy Research*, *8*. https://doi.org/10.3389/fenrg.2020.608586

[2] Powers, M. L. (1990). Analysis off Gravity Separation in Freewater Knockouts. *SPE Production Engineering*, *5*(01), 52–58. https://doi.org/10.2118/18205-PA

[3] PANDIELLA, S. S., GARCÍA, L. A., DÍAZ, M., & WEBB, C. (1999). SIMULATION OF A TWO PHASE FLOW BY CFD: ANALYSIS OF THE COMPUTATIONAL METHOD. *Chemical Engineering Communications*, *173*(1), 197–214. https://doi.org/10.1080/00986449908912784

[4] de Araújo, C. A. O., Scheid, C. M., Loureiro, J. B. R., Klein, T. S., & Medronho, R. A. (2020). Hydrocylone for oil-water separations with high oil content: Comparison between CFD simulations and experimental data. *Journal of Petroleum Science and Engineering*, *187*, 106788. https://doi.org/10.1016/j.petrol.2019.106788

[5] Kareem, H. J., Hasini, H., & Abdulwahid, M. A. (2023). Investigation of flow regimes, pressure drop, void fraction, film thickness, friction factor and production of two-phase flow in a perforated horizontal wellbore. *Geoenergy Science and Engineering*, *229*, 212099. https://doi.org/10.1016/j.geoen.2023.212099

[6] Shoghl, S. N., Naderifar, A., Farhadi, F., & Pazuki, G. (2021). Optimization of separator internals design using CFD modeling in the Joule-Thomson process. *Journal of Natural Gas Science and Engineering*, *89*, 103889. https://doi.org/10.1016/j.jngse.2021.103889

[7] Behin, J., & Azimi, S. (2015). Experimental and Computational Analysis on Influence of Water Level on Oil-Water Separator Efficiency. *Separation Science and Technology*, *50*(11), 1695–1700. https://doi.org/10.1080/01496395.2014.986332

[8] Fangyuan, M., Youjun, T., & Xian, Y. (2022). Study on multiphase flow field in Falcon separator by CFD simulation. *International Journal of Coal Preparation and Utilization*, *42*(10), 3155–3172. https://doi.org/10.1080/19392699.2021.1946799

[9] Unni, M. P., Chandra, M. G., & Kumar, A. A. (2017). Memory reduction for numerical solution of differential equations using compressive sensing. *2017 IEEE 13th International Colloquium on Signal Processing & Its Applications (CSPA)*, 79–84. https://doi.org/10.1109/CSPA.2017.8064928

[10] Afolabi, E. A., & Lee, J. G. M. (2014). An Eulerian-Eulerian CFD Simulation of Air-Water Flow in a Pipe Separator. *The Journal of Computational Multiphase Flows*, *6*(2), 133–149. https://doi.org/10.1260/1757-482X.6.2.133

[11] Zhang, Y., Qiao, P., Hu, Z., Chen, J., Liu, M., & Peng, S. (2024). Design of an axial hydrocyclone for preliminary water separation using CFD, RSM, and SUS. *Chemical Engineering Research and Design*, *204*, 193–200. https://doi.org/10.1016/j.cherd.2024.02.026

[12] Khatir, Z., Hanson, B. C., Fairweather, M., & Heggs, P. J. (2017). *CFD Analysis of Liquid-Liquid Extraction Pulsed Sieve-Plate Extraction Columns* (pp. 19–24). https://doi.org/10.1016/B978-0-444-63965-3.50005-2

[13] Shokrian, A., Mobli, H., Akbarnia, A., Jafari, A., & Mousazade, H. (2018). Application an Euler-Euler Multiphase-Flow Model for Simulation Flow in a Centrifugal Separator Machine. *American Journal of Fluid Dynamics*, *8*, 112–115. https://doi.org/10.5923/j.ajfd.20180804.02

[14] Ding, H., Zhang, Y., Yang, Y., & Wen, C. (2023). A modified Euler-Lagrange-Euler approach for modelling homogeneous and heterogeneous condensing droplets and films in supersonic flows. *International Journal of Heat and Mass Transfer*, *200*, 123537. https://doi.org/10.1016/j.ijheatmasstransfer.2022.123537

[15] Feng, X., Stewart, S., Sartori, L., & Hodges, K. (2020). Understanding the effect of skim oil recycle on the water/oil separation in steam assisted gravity drainage operations. *Journal of Petroleum Science and Engineering*, *192*, 107233. https://doi.org/10.1016/j.petrol.2020.107233

[16] Qi, H., Shang, X., Zhang, X., Wang, Q., Meng, F., Liang, Z., & Liang, S. (2024). Numerical simulation of oil-water separation in sedimentation tank based on CFD-PBM model. *Energy Sources, Part A: Recovery, Utilization, and Environmental Effects*, *46*(1), 3902–3917. https://doi.org/10.1080/15567036.2024.2325055

[17] Shang, X., Wan, M. P., Ng, B. F., & Ding, S. (2020). A CFD-sectional algorithm for population balance equation coupled with multi-dimensional flow dynamics. *Powder Technology*, *362*, 111–125. https://doi.org/10.1016/j.powtec.2019.11.084

[18] Krepper, E., Frank, T., Lucas, D., Prasser, H.-M., & Zwart, P. (2007). *Inhomogeneous MUSIG Model - a Population Balance Approach for Polydispersed Bubbly Flows*.

[19] Berrio, J. C., Pinilla, A., & Ratkovich, N. (2021). CFD study of oil-water segregated and dispersed flow coalescence in horizontal pipes. *Chemical Engineering Communications*, *208*(12), 1695–1710. https://doi.org/10.1080/00986445.2020.1813116

[20] Wilcox, D. C. (2006). *Turbulence Modeling for CFD* (3rd ed.). D C W Industries.

[21] Chen, J., Anastasiou, C., Cheng, S., Basha, N. M., Kahouadji, L., Arcucci, R., Angeli, P., & Matar, O. K. (2023). Computational fluid dynamics simulations of phase separation in dispersed oil-water pipe flows. *Chemical Engineering Science*, *267*, 118310. https://doi.org/10.1016/j.ces.2022.118310

[22] Shaheed, R., Mohammadian, A., & Kheirkhah Gildeh, H. (2019). A comparison of standard k–ε and realizable k–ε turbulence models in curved and confluent channels. *Environmental Fluid Mechanics*, *19*(2), 543–568. https://doi.org/10.1007/s10652-018-9637-1

[23] García-Ramos, F., Malón, H., Aguirre, A., Boné, A., Puyuelo, J., & Vidal, M. (2015). Validation of a CFD Model by Using 3D Sonic Anemometers to Analyse the Air Velocity Generated by an Air-Assisted Sprayer Equipped with Two Axial Fans. *Sensors*, *15*(2), 2399–2418. https://doi.org/10.3390/s150202399

[24] Grace, J. R., & Taghipour, F. (2004). Verification and validation of CFD models and dynamic similarity for fluidized beds. *Powder Technology*, *139*(2), 99–110. https://doi.org/10.1016/j.powtec.2003.10.006

[25] Gerald, B. (2018). A Brief Review of Independent, Dependent and One Sample t-test. *International Journal of Applied Mathematics and Theoretical Physics*, *4*(2), 50. https://doi.org/10.11648/j.ijamtp.20180402.13

[26] Stern, F., Diez, M., Sadat-Hosseini, H., Yoon, H., & Quadvlieg, F. (2017). Statistical Approach for Computational Fluid Dynamics State-of-the-Art Assessment: N-Version Verification and Validation. *Journal of Verification, Validation and Uncertainty Quantification*, *2*(3). https://doi.org/10.1115/1.4038255

[27] Liang, G., Fu, W., & Wang, K. (2019). Analysis of t- test misuses and SPSS operations in medical research papers. *Burns & Trauma*, *7*. https://doi.org/10.1186/s41038-019-0170-3

[28] Montgomery, D. C., Runger, G. C., & Hubele, N. F. (2010). *Engineering Statistics* (5th ed.). John Wiley & Sons.

[29] Oberkampf, W. L., & Roy, C. J. (2010). *Verification and Validation in Scientific Computing*. Cambridge University Press. https://doi.org/10.1017/CBO9780511760396

[30] Blazek, J. (2006). *Computational Fluid Dynamics: Principles and Applications* (2nd ed.). Elsevier Science.

[31] Je, Y.-W., Kim, Y.-J., & Kim, Y.-J. (2022). The Prediction of Separation Performance of an In-Line Axial Oil–Water Separator Using Machine Learning and CFD. *Processes*, *10*(2), 375. https://doi.org/10.3390/pr10020375

[32] Acharya, T., & Casimiro, L. (2020). Evaluation of flow characteristics in an onshore horizontal separator using computational fluid dynamics. *Journal of Ocean Engineering and Science*, *5*(3), 261–268. https://doi.org/10.1016/j.joes.2019.11.005

[33] Pourahmadi Laleh, A., Svrcek, W. Y., & Monnery, W. D. (2012). Design Criteria for Oilfield Separators Improved by Computational Fluid Dynamics. *Chemical Engineering & Technology*, *35*(2), 323–333. https://doi.org/10.1002/ceat.201100351

[34] Buhamad, A., & Saeedi Dehaghani, A. H. (2023). Performance evaluation of downhole oil–water separators in wells that use DWL technique using computational fluid dynamics: influence of velocities and flow rates. *Journal of Petroleum Exploration and Production Technology*, *13*(11), 2237–2249. https://doi.org/10.1007/s13202-023-01671-w

[35] Ahmed, T., Russell, P. A., Hamad, F., & Gooneratne, S. (2019). Experimental Analysis and Computational-Fluid-Dynamics Modeling of Pilot-Scale Three-Phase Separators. *SPE Production & Operations*, *34*(04), 805–819. https://doi.org/10.2118/197047-PA

[36] Shinde, P., Kothmire, P., & Bhalerao, Y. (2020). CFD Investigation on Fluid Flow Analysis in Fluid Separator. In *Techno-Societal 2018* (pp. 131–141). Springer International Publishing. https://doi.org/10.1007/978-3-030-16962-6_14

[37] Zhu, M., Hu, D., Xu, Y., & Zhao, S. (2020). Design and Computational Fluid Dynamics Analysis of a Three-Phase Decanter Centrifuge for Oil-Water-Solid Separation. *Chemical Engineering & Technology*, *43*(5), 1005–1015. https://doi.org/10.1002/ceat.201900245

[38] Pourahmadi Laleh, A., Svrcek, W. Y., & Monnery, W. (2013). Computational Fluid Dynamics-Based Study of an Oilfield Separator--Part II: An Optimum Design. *Oil and Gas Facilities*, *2*(01), 52–59. https://doi.org/10.2118/161036-PA

[39] Kim, S., Kim, H., Jeong, H. S., & Kim, Y. (2025). Optimal design of perforated baffles for enhancing oil-water separation performance using genetic algorithms. *Results in Engineering*, *26*, 104668. https://doi.org/10.1016/j.rineng.2025.104668

[40] Zhou, G., Wang, J., Song, R., Xu, C., & Wang, P. (2022). Experimental study on droplet breakup and droplet particles diffusion of a pressure nozzle based on PIV. *Chemical Engineering Science*, *258*, 117737. https://doi.org/10.1016/j.ces.2022.117737

[41] Zhang, J., Liang, P.-F., & Liu, Y.-Z. (2024). Liquid breakup and droplets behavior of free triple-impinging jets with different impinging distance. *Chemical Engineering Journal*, *500*, 156984. https://doi.org/10.1016/j.cej.2024.156984

[42] Kirar, P. K., Kumar, N., & Sahu, K. C. (2024). Dynamics of jet breakup and the resultant drop size distribution-effect of nozzle size and impingement velocity. *Physics of Fluids*, *36*(10). https://doi.org/10.1063/5.0225452

[43] Pun, K., Hamad, F., Pun, M., Lawson, G., & Russell, P. (2024). Experimental investigation of the effect of slenderness ratio and retention time on the separation performance of a two-phase horizontal separator. *Chemical Engineering Research and Design*, *207*, 221–231. https://doi.org/10.1016/j.cherd.2024.05.035

[44] Pun, K., Hamad, F., Ahmed, T., Ugwu, J., Najim, S., Eyers, J., Lawson, G., & Russell, P. (2023). Experimental investigation of the parameters that affect droplet size and distribution for design calculations of two-phase separators. *Heliyon*, *9*(4), e15397. https://doi.org/10.1016/j.heliyon.2023.e15397

[45] Chen, X., Zheng, J., Jiang, J., Peng, H., Luo, Y., & Zhang, L. (2022). Numerical Simulation and Experimental Study of a Multistage Multiphase Separation System. *Separations*, *9*(12), 405. https://doi.org/10.3390/separations9120405

[46] Pinilla, J. A., Guerrero, E., Pineda, H., Posada, R., Pereyra, E., & Ratkovich, N. (2019). CFD modeling and validation for two-phase medium viscosity oil-air flow in horizontal pipes. *Chemical Engineering Communications*, *206*(5), 654–671. https://doi.org/10.1080/00986445.2018.1516646

[47] Zhang, S., Zhao, L., Zhou, L., Liu, L., & Jiang, M. (2023). Numerical and experimental study on enhanced oil–water separation performance using hydrocyclone coupled with particles. *Physics of Fluids*, *35*(11). https://doi.org/10.1063/5.0177823